Arabian Journal for Science and Engineering (2021) 46:4703–4717
https://doi.org/10.1007/s13369-020-05118-w

RESEARCH ARTICLE-CIVIL ENGINEERING

A Hybrid of Firefly and Biogeography-Based Optimization Algorithms for Optimal Design of Steel Frames

Hamid Farrokh Ghatte[1]

Received: 1 July 2020 / Accepted: 5 November 2020 / Published online: 24 November 2020

Abstract
The principle purpose of the current study is to hybridize firefly algorithm (FA) as a nature-inspired meta-heuristic developed based on the flashing patterns and biogeography-based optimization (BBO) to present a qualified algorithm in the case of optimization of steel frame (SF) structures. In the proposed meta-heuristic algorithm, FA works as a global search engine while BBO achieves the local search task. The proposed algorithm is termed as a firefly algorithm–biogeography-based optimization (FA–BBO). FA–BBO algorithm was employed for the optimization of benchmark SF problems for the validity in the case of a new algorithm. The numerical outputs demonstrate that the new FA–BBO algorithm presents a better computational performance in the comparison of the current algorithms.

Keywords Biogeography-based optimization · Firefly algorithm · Meta-heuristic · Optimization steel structures

1 Introduction

Design of the structures with minimum weight or minimize an objective function value based on the minimal cost of the structures, regarding the design criteria, is the main purpose for structural optimization [1–5]. Mathematical programming methods have widely been applied in solid and structural optimization [6–9]. During the past few decades, several optimization algorithms have been improved for different structural systems like truss and steel frame (SF) structures [10–18]. As well as, the performance-based design of SFs utilizing meta-heuristic optimization algorithms has been developed by the researchers [19–21]. The meta-heuristic algorithms have remarkable characteristics that vary from the gradient-based methods. This class of optimization methods not only demands no gradient computations but also they are straightforward for computer programming. Employing meta-heuristic algorithms allows exploration of a further fraction of the design space in comparison with gradient-based optimization methods. The meta-heuristics illustrate the effectiveness of numerous optimized structural issues like SFs or truss [22–26]. Many researchers employed popular meta-heuristics such as genetic algorithms (GA), particle swarm optimization (PSO), ant colony optimization (ACO) and harmony search (HS) for the optimization of structural systems. In the present study, the firefly algorithm (FA) [27], biogeography-based optimization (BBO) [28] and their combination are focused.

FA is a recently developed nature-inspired meta-heuristic based on the flashing patterns and behavior of fireflies. Additionally, FA is more efficient in comparison with other design optimization strategies since requires a lower output of evaluations for function. Moreover, FA has certain defects, for instance trapping to the local optimization results in the case of a complex searching space as well as a disability to do an excellent local search near the local optimum. The common knowledge that the BBO may carry out superior to the other meta-heuristic optimization strategies through the initial iterations, but in the case of increasing the number of iterations, it does not available competitive. BBO was encouraged based on biogeography, which refers to geographical distribution. In the current work, an unused optimization algorithm is represented by a combination of FA and BBO for the optimization of SF structures. The optimization procedure is performed by BBO around the optimum alternative found by FA to finely investigate the design space. As long as the algorithm is a serial integration of FA and BBO it is denoted as FA–BBO meta-heuristic. In this paper, the design variables are areas for the cross section of the struc-

✉ Hamid Farrokh Ghatte
ghatte@itu.edu.tr; hamid.ghatte@antalya.edu.tr

[1] Civil Engineering Department, Faculty of Engineering, Antalya Bilim University, Antalya, Turkey

tural elements and the design constraints are imposed on the nodal displacements and element stresses. The numerical output demonstrates the effectiveness and productiveness of FA–BBO against the FA and BBO.

2 Optimization Problem Formulation

For optimal design of an SF including *ne* members accumulated in *ng* design sets, the design variables of any design set are usually chosen based on the standard profile list. In this case, the optimization problem can be formulated in the following way:

$$\text{Minimize: } w(X) = \sum_{i=1}^{ng} \rho_i A_i \sum_{j=1}^{nm} L_j \tag{1}$$

$$\text{Subject to: } g_k(X) \le 0, \quad k = 1, 2, \ldots, nc \tag{2}$$

$$X = \{ x_1 \; x_2 \; \ldots \; x_i \; \ldots \; x_{ng} \}^{\mathrm{T}} \tag{3}$$

in this equations; *xi* presents an integer number to express the sequence of steel cross sections for the *i*th group; *w* is the frame weight, the weight per unit volume and area of the cross sections are presented by ρ_i, and A_i, respectively, for the *i*th group section; the number of the elements is presented by *nm* that accumulated through the *i*th set; for the *j*th element in the *i*th set L_j presented as a length of the elements; the *k*th behavioral constraint represented by g_k.

The lateral inter-story drift ratio can be considered as follows:

$$g_{d,l} = \frac{\theta_l}{R_I} - 1 \le 0, \quad l = 1, \ldots, ns \tag{4}$$

where Θ_l is the drift ratio for the inter-story; the inter-story drift ratio index represented by R_l authorized based on the code of practice and *ns* is the overall number of stories.

The demand-capacity ratio (DCR) constraints of structural elements exposed to axial load as well as flexural stresses are computed in the following way [29]:

$$\text{DCR} = \begin{cases} \left[\frac{P_u}{2\phi_c P_n} + \left(\frac{M_{ux}}{\phi_b M_{nx}} + \frac{M_{uy}}{\phi_b M_{ny}} \right) \right] & \text{if } \frac{P_u}{\phi_c P_n} < 0.2 \\ \left[\frac{P_u}{\phi_c P_n} + \frac{8}{9} \left(\frac{M_{ux}}{\phi_b M_{nx}} + \frac{M_{uy}}{\phi_b M_{ny}} \right) \right] & \text{if } \frac{P_u}{\phi_c P_n} \ge 0.2 \end{cases} \tag{5}$$

$$g_{\text{DCR},m} = \text{DCR}_m - 1 \le 0, \quad m = 1, \ldots, ne \tag{6}$$

in these equations P_u presents the required strength; P_n presents the nominally axial compression or tension strength; $\emptyset_c$ presents the resistance coefficient; M_{ux} and M_{uy} present the essential flexural strengths through the *x* and *y* directions; M_{nx} and M_{ny} present the nominal flexural strengths through the *x* and *y* directions, and $\emptyset_b = 0.9$ is the reduction factor of flexural resistance.

In the present work, the exterior penalty function method (EPFM) [30] is used to handle the design constraints. Using EPFM converts the main constrained optimization problem into an unconstrained one. Therefore, the pseudo unconstrained objective function may be presented through the following equation:

$$\Psi(X, r) = w(X) \left(1 + r \sum_{l=1}^{ns} (\max\{0, g_{d,l}\})^2 + r \sum_{m=1}^{ne} (\max\{0, g_{\text{DCR},m}\})^2 \right) \tag{7}$$

in this equation Ψ present, the pseudo-objective function and *r* present a penalty parameter. For minimizing the above-mentioned pseudo-objective function, several popular meta-heuristics are employed in the present study. The theoretical background of the meta-heuristics is explained in the next section.

3 Meta-heuristic Algorithms

The main idea that supports designing the meta-heuristic algorithms is to tackle complex optimization issues when the other optimization methods have failed to be effective. Meta-heuristics are applied to a very wide range of problems and they mimic natural metaphors to solve complex optimization problems. In this study, FA and BBO are utilized for discovering the optimum design of SFs subject to static loading.

3.1 Firefly Algorithm

The FA is a relatively new meta-heuristic optimization algorithm that was proposed by Yang at Cambridge University in 2008 according to the inspired by the flashing behavior of fireflies [31]. Fireflies communicate, search for prey and find mates employing bioluminescence with varied flashing models [32]. By considering the previous investigations, it may be considered that in almost all areas of engineering FA can be employed as a powerful optimization tool [33–39]. To develop the FA, natural flashing specifications of fireflies have been employed based on the following rules [27]:

a. The fireflies are unisex; consequently, one firefly will be attracted to other fireflies irrespective of the sex.
b. The attractiveness of any firefly is proportional to its brightness; therefore, for every two flashing fireflies, the less brightness of the firefly will move toward the brighter one. The attractiveness is proportional to the brightness and by increasing the distance the brightness

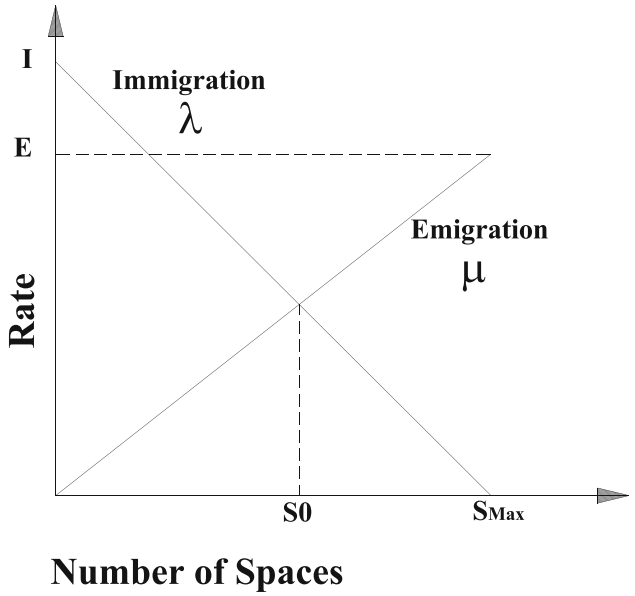

Fig. 1 The linear model of migration [44]

will decrease. It will move randomly when there is no brighter firefly than the particular one.

c. The brightness for a firefly is obtained based on the nature of the objective function.

Firefly attractiveness is obtained based on its brightness or light intensity that is determined following the objective function of the optimization problem. Nevertheless, β (the attractiveness) that depends on the judgment of the beholder defers based on the distance between two fireflies. β can be presented in the following way [31]:

$$\beta = \beta_0 e^{-\gamma \cdot r^2} \tag{8}$$

in this equation r is the distance between two fireflies, β_0 is the attractiveness for $r = 0$, and γ is the light absorption factor.

The distance between fireflies i and fireflies j at corresponding X_i and X_j is obtained employing the following equation:

$$r_{ij} = \left\| X_i - X_j \right\| = \sqrt{\sum_{k=1}^{d} (x_{i,k} - x_{j,k})^2} \tag{9}$$

in this equation $x_{i,k}$ is the kth parameter of the spatial coordinate x_i.

In the FA, the firefly i movement toward a brighter firefly j is obtained by the following equation:

$$X_i = X_i + \beta_0 e^{-\gamma \cdot r_{ij}^2} (X_j - X_i) + \alpha(\text{rand} - 0.5) \tag{10}$$

in this equation, the second term belongs to the attraction. Additionally, the randomization parameter is represented by α where the rand is a randomly generated number that distributed in the uniform condition in [0, 1].

3.2 Biogeography-Based Optimization

Simon represented the BBO algorithm in 2008 as a certain feature algorithm in common with other biology-based algorithms [28]. In this algorithm, the main concept was inspired based on the biogeography, that relates to the biological organisms in terms of time and space. As a reliable approximation of many engineering issues, the BBO algorithm has been employed [40–42]. The different islands, centuries, lands, or even continents over decades, or millennia are the case studies of these investigations. The different ecosystems in terms of habitats or territories are evaluated to figure out the relationships between various species (habitants) in the case of immigration, emigration and mutation. The progress in ecosystems to achieve a stable situation based on the different types of predators and prey and the efficiency of migration and mutation was the major inspiration in BBO [28].

BBO employs several search agents called habitats. These habitats are analogous to fireflies in FA. The BBO algorithm assigns each habitat a vector of habitants suitability index (HSI) defines the overall fitness of a habitat. The higher the HSI, the more fit the habitat. The habitats evolve based on three main rules in the following ways [43]:

1. The high HSI habitats living in habitants that are more likely to emigrate to habitats by the low HSI.
2. The low HSI habitats more prone to attract new immigrant habitants from those with high HSI.
3. Regardless of their HSI values, the habitats might be facing the random changes in the habitants.

In nature, these concepts bring a balance between different ecosystems. In other words, nature tends to improve the overall stability of different geographical regions. The BBO algorithm utilizes these concepts to improve the HSI of all habitats, which results in changing the primary random solutions for particular problems. The employed BBO algorithm starts with a random set of habitats. Each habitat has ng different habitants that correspond to the design variables number of a particular problem. Besides, each habitat has its immigration, emigration and mutation rates. This mimics the characteristic of various geographically separated locations in nature.

The components of the biography model and their correspondence based on the BBO algorithm in terms of the optimization point of view represented in the following ways [44]:

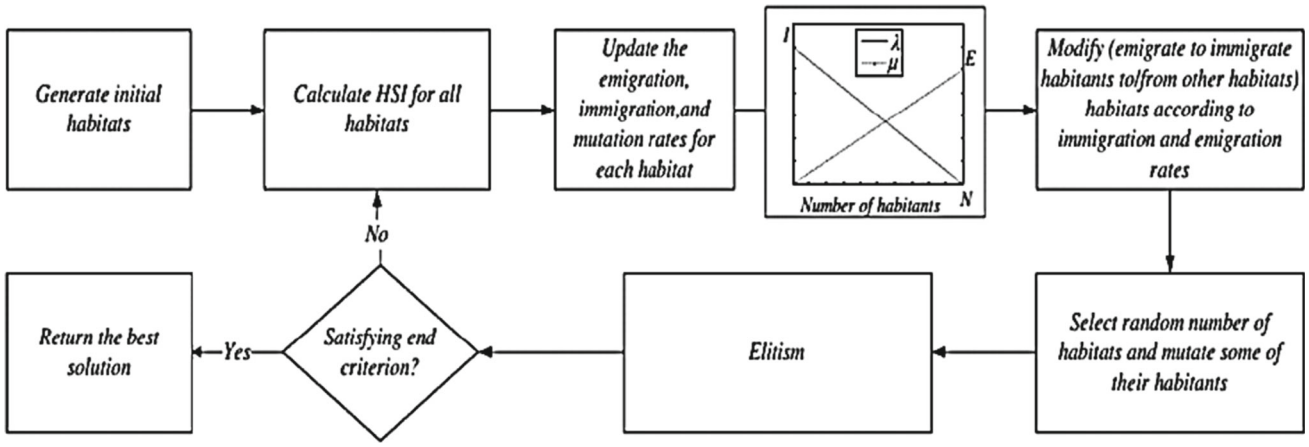

Fig. 2 General steps of the BBO algorithm

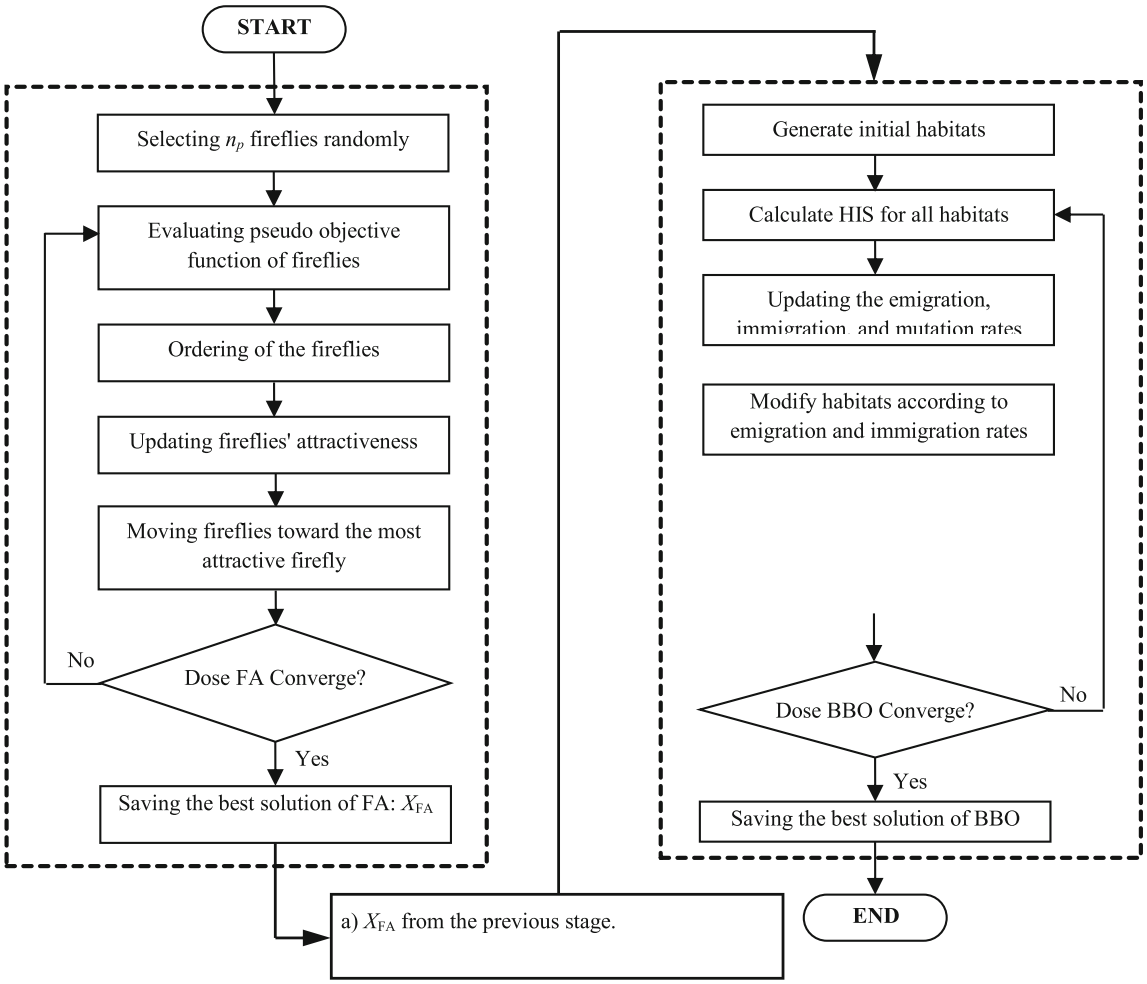

Fig. 3 Flowchart of the proposed algorithm

- Habitat (H): Habitat presents a solution within the search space of a d-dimensional numerical optimization problem.
- Habitat Suitability Index (HSI): Throughout a biography pattern, the geographical areas, that are well investigated as residences for biological species are with a high value of HSI.
- Suitability Index Variables (SIV): The computation of the HSI amount is affecting through the additional coefficients

for instance rainfall, diversity of vegetation, land area as well as temperature, that they called the SIVs.

- Immigration Rate: The criterion is devoted to controlling the immigration habitat. The maximum amount of the immigration amount in a habitat is achieved when the species are not inside of the habitat.
- Emigration Rate: The μ criterion is controlling the habitat emigration. The emigration will be null when there are no species. By increasing the number of spaces, species can leave their habitat to explore other residences. The maximum emigration rate (E) is achieved through a habitat in the case of containing the maximum amount of species that can support it.
- Migration model: Based on the various mathematical patterns for biogeography, different migration curves might be utilized. A linear model is represented in Fig. 1. In this figure, S0 is the equilibrium number of species, by consideration of an equal amount for the immigration and emigration rates. The maximum possible immigration rate represented by I, where the maximum possible emigration rate is represented by E, and the greatest possible amount of species that the habitat might support is represented by $S_{\max}$.

Emigration (μ_k) and immigration (λ_k) are formulated as functions of the habitants number in the following way [43]:

$$\mu_k = \frac{E \cdot n}{N} \tag{11}$$

$$\lambda_k = \left(\frac{1-n}{N}\right) \cdot I \tag{12}$$

in this equation, n is the current number of habitants, N is the allowed maximum number of habitants.

These latter two rates are depicted in Fig. 2. It can be inferred from this figure that a high number of habitants coincides with a high probability of emigration and a low probability of immigration [43].

The third component in BBO, mutation, improves the exploration of BBO as well as maintains habitats. The component is illustrated in the following ways [43]:

$$m_n = M \cdot \left(\frac{1-P_n}{P_{\max}}\right) \tag{13}$$

in this equation, the initial value for mutation is M that is defined by the user p_n is the mutation probability belongs to nth habitat, and $p_{\max} = \text{argmax}\,(p_n)$, n=1,2, …, N.

The global levels of the BBO algorithm are represented within Fig. 3 as a flowchart. Figure 2 demonstrates that the BBO algorithm initiates by random groups of habitats. Subsequently of obtaining the HSI of any habitat, the emigration, immigration and mutation ratios are upgraded. Based on these ratios, the non-elite habitants are migrated and mutated. For use as the next elites generation, a predefined amount of the best habitats is rescued. Lastly, the algorithm of BBO is concluded based on the satisfaction of a termination criterion. The elitism prevents the best solutions out to become corrupted with immigration. Therefore, some of the best habitats at any iteration are retained. Consequently, if their HSI is ruined based on the mutation, then the best solutions might be covered [43].

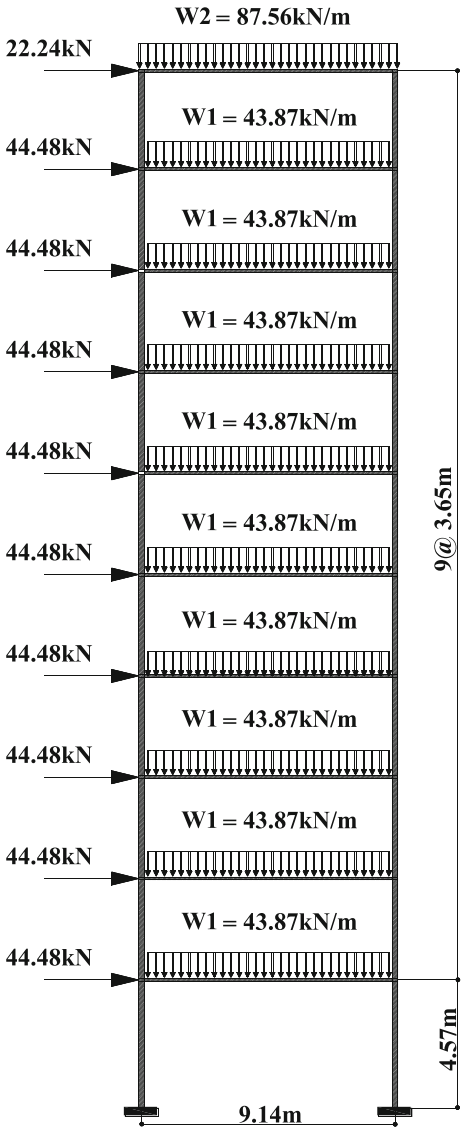

Fig. 4 10-story steel frame

3.3 FA–BBO Algorithm

One of the defects known in FA is that all fireflies in final iterations converge to the more attractive firefly and therefore the algorithm converges to local optima and this is a reason that FA incapacitates for doing a proper local search. Con-

Table 1 Optimal results of 10-story steel frame

Element groups	Pezeshk et al. [45]	Kaveh et al. [22]	Camp et al. [46]	Present work		
				FA	BBO	FA–BBO
Beam 1–3S	W33 × 118	W33 × 118	W30 × 108	W33 × 118	W33 × 118	W33 × 118
Beam 4–6S	W30 × 90	W30 × 90	W30 × 90	W30 × 90	W30 × 99	W30 × 90
Beam 7–9S	W27 × 84	W24 × 76	W27 × 54	W24 × 84	W27 × 84	W24 × 84
Beam 10S	W24 × 55	W14 × 30	W21 × 44	W24 × 68	W24 × 62	W21 × 44
Column 1–2S	W14 × 233	W14 × 233	W14 × 233	W14 × 233	W14 × 211	W14 × 211
Column 3–4S	W14 × 176	W14 × 176	W14 × 176	W14 × 159	W14 × 159	W14 × 159
Column 5–6S	W14 × 159	W14 × 145	W14 × 145	W14 × 132	W14 × 132	W14 × 145
Column 7–8S	W14 × 99	W14 × 90	W14 × 99	W14 × 90	W14 × 90	W14 × 90
Column 9–10S	W12 × 79	W12 × 65	W12 × 65	W14 × 61	W14 × 61	W14 × 61
Weight (KN)	289.72	274.99	278.48	275.44	272.95	269.75
Number of analyses	3690	2500	8300	4000	4000	4000

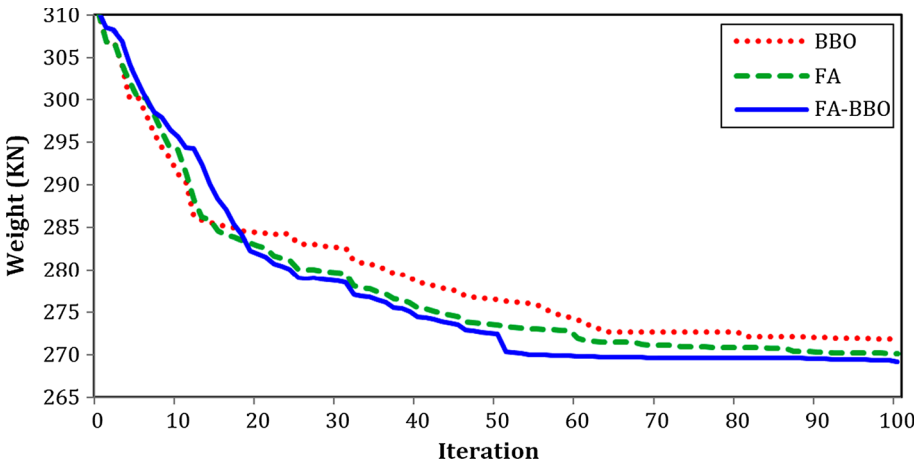

Fig. 5 Convergence histories of FA, BBO and FA–BBO for 10-story steel frame optimization

sidering the local search ability of FA is relatively poor and the local search ability of BBO is appropriate in comparison with FA. Therefore, FA and BBO are serially integrated to overcome the aforementioned difficulty.

To resolve the problem for improving the performance of the optimization process for finding a near-global solution, FA and BBO are serially integrated and this results in an algorithm termed an FA–BBO algorithm. The proposed FA–BBO meta-heuristic is a two-stage algorithm. In the first stage, a preliminary optimization is performed by FA to explore the design space by performing a limited number of iterations (say n1). The optimum solution found by FA is termed XFA. In the second stage, a normal finer search is implemented about the XFA by employing BBO again by performing a limited number of iterations (say n2). The initial population of the FA is randomly selected from all over the design space while the optimal initial population of BBO is selected as follows: X_{FA} is directly transformed to the optimal initial population and the rests, say X_{rndi}, be chosen using the following equation:

$$X_j = \mathrm{N}(X_{\mathrm{FA}}, \gamma X_{\mathrm{FA}}), \quad j = 1, 2, \ldots, (n-1) \tag{14}$$

where the randomly normal distributed vector is represented by **N** with a mean of X_{FA} with a standard deviation of γX_{FA}.

The γ coefficient has a critical role in the case of the convergence of the algorithm. In the current study, different values are investigated for γ where the optimal performance is achieved for the value of $\gamma = 0.1$. The flowchart of the proposed algorithm is represented in Fig. 3.

4 Numerical Results

For evaluation of the presented algorithm, three benchmarks, SF optimization problems are represented and the outputs are controlled based on the existing reports in the literature. W-shaped (from the standard profile list) cross sections were employed for all of the members. For each design example,

25 independent optimization runs have been performed and the best design is reported.

4.1 Example 1: 10-Story Planar SF

Figure 4 represents a 10-story SF, where the module of elasticity is 200 GPa and the yield stress of the material is 248.2 MPa. Moreover, the effective length factors of the members are obtained as $K_x = 0$ for a sway-permitted frame and the out-of-plane effective length factor is specified as $K_y = 1$. Any of the columns is considered unbraced through the length and one-fifth of the length of any span has been considered as unbraced length. The lateral inter-story drift ratio is limited by $h/300$ (h is the story height).

Fabrication conditions are required for the element constructions of the frame. The same cross section for beams was employed for three beginning stories from the foundation. Furthermore, the same cross section for columns is employed for any two consecutive stories. Four cross sections for beams and five cross sections for columns resulting in the element grouping in nine design variables. The cross section for beam element sets is selected from the 267 W-shaped cross sections. The column sections are restricted to W14 and W12 (from the standard profile list). For all of the applied meta-heuristics, the population size is 40 and the upper limitation for iterations was 100. In the framework of FA–BBO, the number of iterations for preliminary optimization by FA and BBO is equal to 50 (i.e., $n1 = n2 = 50$). The outputs for the optimization are presented in Table 1.

The results show that FA–BBO outperforms the algorithms applied in [46, 47]; moreover, the optimal solution found by FA–BBO is 2.06% and 1.17% lighter than those of FA and BBO. Figure 5 shows the convergence histories of FA, BBO and FA–BBO indicating that the FA–BBO possesses a better convergence rate compared with FA and BBO.

For the optimal solution found by FA–BBO, the drift ratio for inter-story and element stress ratios are shown in Figs. 6 and 7, respectively. The outputs present a feasible solution.

4.2 Example 2: 24-Story Planar SF

A 24-story frame with a grouping of the details of the elements is considered and represented in Fig. 8. In this example, $E = 205$ GPa and $Fy = 230.3$ MPa. The factors for the effective length of the members are obtained as $K_x = 0$ for a sway-permitted frame and the out-of-plane effective length factor is considered as $K_y = 1$. All of the members in terms of beams and columns are specified as unbraced elements along the lengths.

A H/300 limitation was considered for the maximum lateral displacement and h/300 was considered as a limitation of the maximum inter-story drift ratio. In this formulations, the

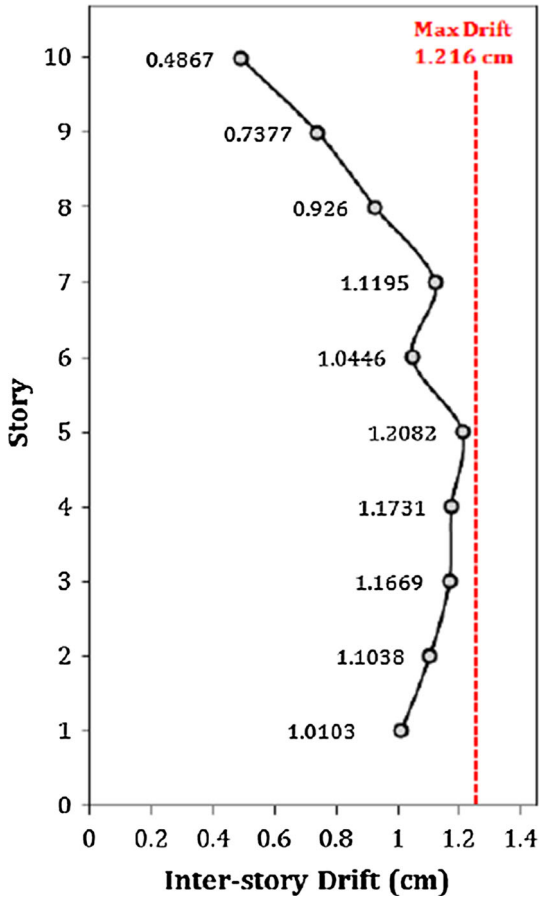

Fig. 6 Inter-story drift profile for optimal 10-story steel frame based on FA–BBO

height of the building represented by H and the height of one story represents by h. Fabrication conditions are imposing the construction of the 168-element frame demands the same cross section of the beam utilized through the first as well as the third bay on any floors (exclude the roofs), resulting in the scope of four groups of beams. The exterior columns teaming up into one group at the beginning of the foundation, where the interior columns teaming up in another set over three consecutive stories. 16 cross sections for columns and 4 cross sections for beams (20 design variables overall) were the groupings for the results. W-shaped cross sections for the beam element groups are chosen, where the cross section of columns groups is limited to W14 (from the standard profile list). The population size and the upper limitation for the iterations are considered to be 40 and 150, respectively. In the framework of FA–BBO, the number of iterations for preliminary and final optimization processes is equal to 75 (i.e., $n1 = n2 = 75$). Table 2 presents the results of the optimization.

The results indicate that the optimal solution found based on the FA–BBO is better than those found in [27–29]. The weight of the optimal structure found by FA–BBO is 4.31% and 3.34% lighter than those of FA and BBO, respectively.

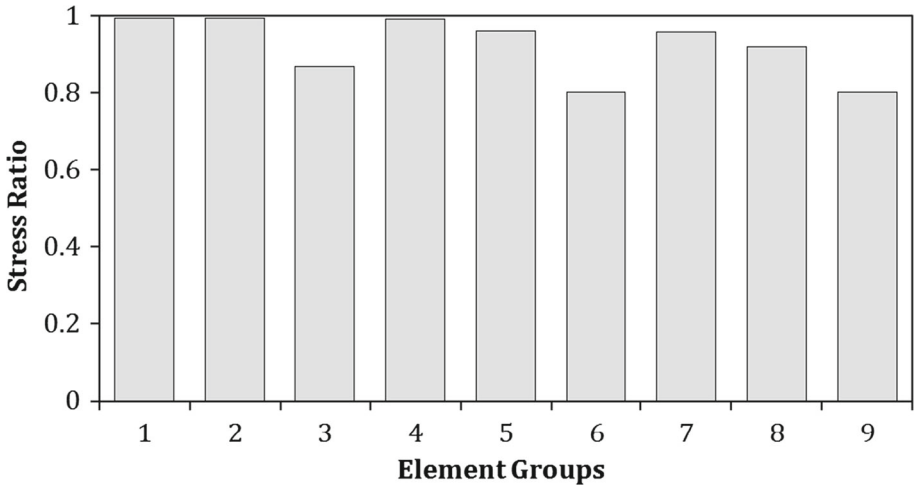

Fig. 7 Element group stress ratios for optimal 10-story steel frame based on FA–BBO

Table 2 Optimal results of 24-story steel frame

Element groups	Camp et al. [46]	Kaveh et al. [22]	Degertekin [47]	Present work		
				FA	BBO	FA–BBO
1	W30 × 90	W30 × 99	W30 × 90	W30 × 99	W30 × 90	W30 × 90
2	W8 × 18	W16 × 26	W10 × 22	W8 × 21	W14 × 22	W12 × 14
3	W24 × 55	W18 × 35	W18 × 40	W18 × 46	W18 × 35	W21 × 48
4	W8 × 21	W14 × 22	W12 × 16	W6 × 9	W8 × 21	W6 × 9
5	W14 × 145	W14 × 145	W14 × 176	W14 × 145	W14 × 145	W14 × 145
6	W14 × 132	W14 × 132	W14 × 176	W14 × 120	W14 × 132	W14 × 120
7	W14 × 132	W14 × 120	W14 × 132	W14 × 109	W14 × 132	W14 × 120
8	W14 × 132	W14 × 109	W14 × 109	W14 × 82	W14 × 132	W14 × 74
9	W14 × 68	W14 × 48	W14 × 82	W14 × 74	W14 × 68	W14 × 68
10	W14 × 53	W14 × 48	W14 × 74	W14 × 61	W14 × 53	W14 × 53
11	W14 × 43	W14 × 34	W14 × 34	W14 × 34	W14 × 38	W14 × 38
12	W14 × 43	W14 × 30	W14 × 22	W14 × 26	W14 × 30	W14 × 22
13	W14 × 145	W14 × 159	W14 × 145	W14 × 109	W14 × 132	W14 × 109
14	W14 × 145	W14 × 120	W14 × 132	W14 × 99	W14 × 132	W14 × 109
15	W14 × 120	W14 × 109	W14 × 109	W14 × 109	W14 × 120	W14 × 109
16	W14 × 90	W14 × 99	W14 × 82	W14 × 90	W14 × 90	W14 × 90
17	W14 × 90	W14 × 82	W14 × 61	W14 × 74	W14 × 74	W14 × 74
18	W14 × 61	W14 × 53	W14 × 48	W14 × 53	W14 × 61	W14 × 68
19	W14 × 30	W14 × 38	W14 × 30	W14 × 34	W14 × 30	W14 × 30
20	W14 × 26	W14 × 26	W14 × 22	W14 × 22	W14 × 22	W14 × 22
Weight (KN)	980.63	967.33	955.74	943.60	934.13	902.92
Number of analyses	30,000	3500	13,924	6000	6000	6000

For the optimal solution found by FA–BBO, the drift ratio for inter-story and element stress ratios are shown in Figs. 9 and 10, respectively. Similarly, in this example, the outputs present a feasible solution.

4.3 Example 3: 20-Story 3D Steel Braced Frame

A 20-story 3D braced SF (see Fig. 11) with 1040 elements are selected based on the study of Hasancebi et al. [48]. In this study, the columns are classified into three-member sets in a story; a corner, interior columns and exterior columns. Additionally, the beams are classified into two sets; interior beams and exterior beams.

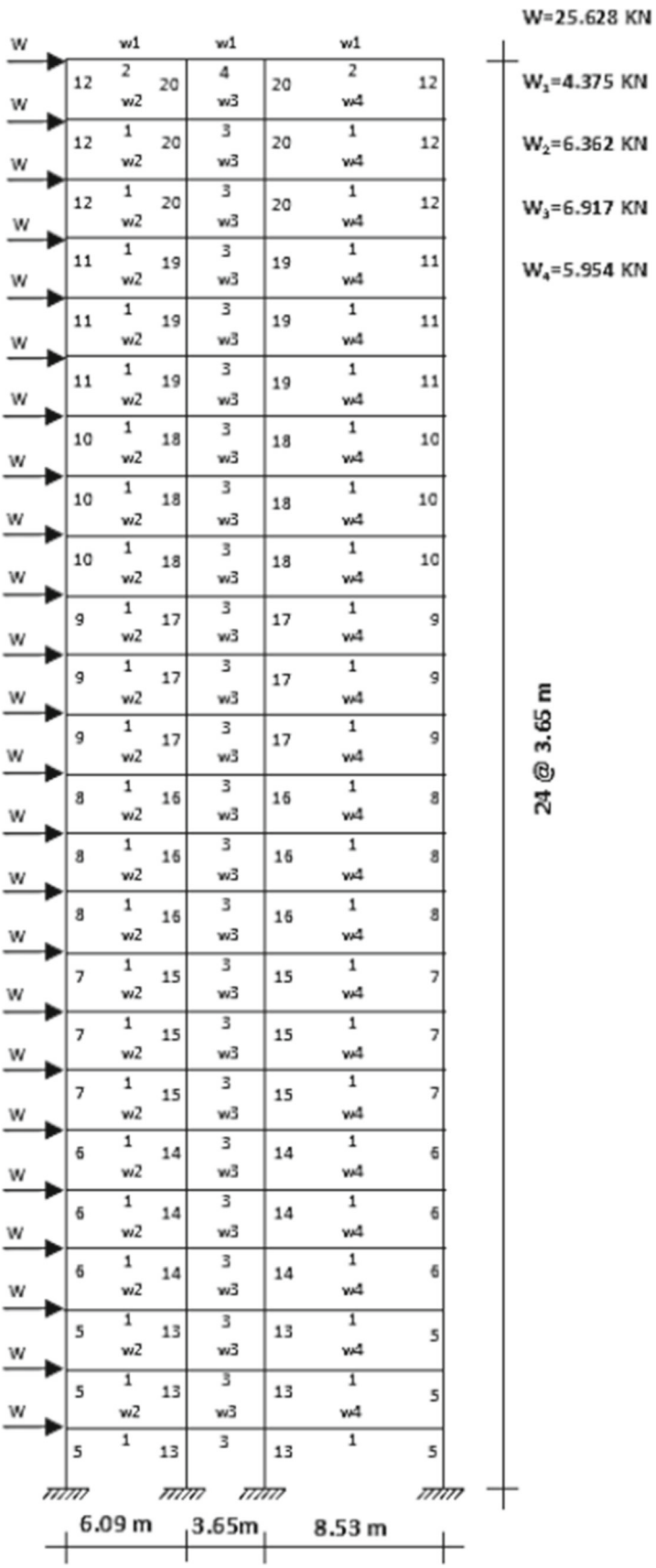

Fig. 8 24-story steel frame

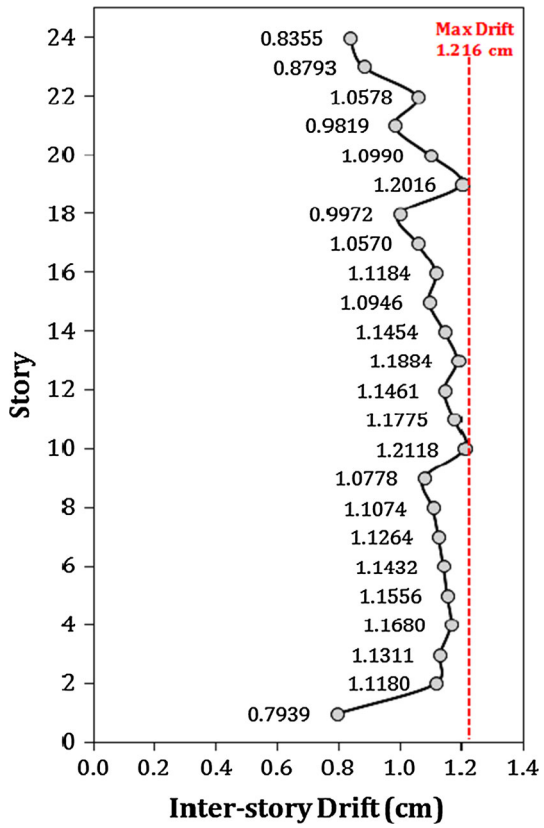

Fig. 9 Inter-story drift profile for optimal 24-story steel frame based on FA–BBO

The corner, interior and exterior columns as well as interior and exterior beams, and bracings are categorized with the same cross section through the two adjacent stories. Therefore, 60 distinct member sets are in the example. ASD-AISC [49] specification is used to control the stress constraints. Additionally, the displacements in x and y directions at joints are limited to 18.29 cm where the maximum amount of inter-story drifts ratio is considered as 0.91 cm. The elastic modulus was considered as 2.039×10^{10} kg/m^2 and the yield stress was considered as 2.531×10^7 kg/m^2 for the used steel. The applied dead and live loads considered from the first to 19th floors are considered 2.88 kN/m^2 and 2.39 kN/m^2, respectively. In the case of the roof, a dead load of 2.88 kN/m^2 and a snow load of 1.20 kN/m^2 were considered. The gravitational loads are utilized as distributed uniform loads through the beams based on the distribution formulations improved for slabs [48]. The wind loads for design are calculated based on ASCE 7-05 [50] as follows [48]:

$$p_{\mathrm{w}} = \left(0.613 K_z K_{zt} K_{\mathrm{d}} V^2 I\right)\left(G C_{\mathrm{p}}\right) \tag{15}$$

in this equation the design wind pressure is represented by p_{w} in terms of kN/m^2, the velocity exposure coefficient is represented by K_z, the topographic factor represented by K_{zt}, the direction factor of wind reprinted by K_{d}, the basic speed for wind represented by V, the gust factor represented by G and the coefficient for external pressure represented by C_{p}. Based on the parameters that have been used by Hasancebi et al. [48], the buildings are considered in a flat terrain location with $V = 46.94$ m/s and exposure category B and the following values: $K_{zt} = 1.0$, $K_{\mathrm{d}} = 0.85$, $I = 1.0$, $G = 0.85$ and $C_{\mathrm{p}} = 0.8$ for windward facing and 0.5 for leeward facing. After the calculation of the wind loads, the load is acting in the uniform condition at each level of the floors. A combination of the gravity and wind loads is considered into two types of loading conditions based on the wind loads acting along the x-axis or the y-axis [48].

To implement the optimization process, the population size is chosen to be 50 and the maximum number of iterations is limited to 400. For FA–BBO meta-heuristic, the number of iterations for each of FA and BBO meta-heuristics is limited to 200 (i.e., $n1 = n2 = 200$). Table 3 presents the optimization results.

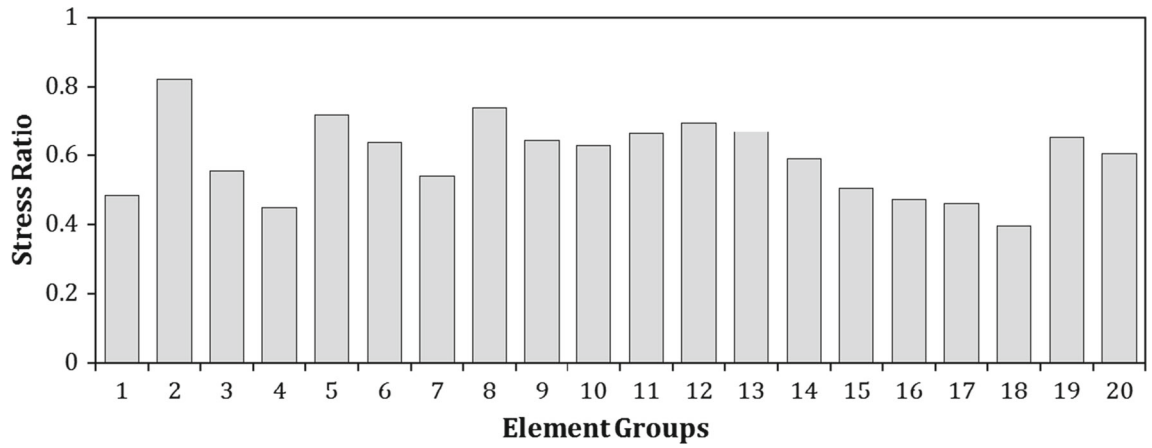

Fig. 10 Element group stress ratios for optimal 24-story steel frame based on FA–BBO

Table 3 Optimal results of 20-story 3D steel frame

Members	Story no.	Group no.	Hasancebi et al. [48]	Present work		
				FA	BBO	FABBO
Exterior beam	1–2	1	W8 × 18	W12 × 40	W16 × 31	W14 × 22
	3–4	2	W10 × 22	W12 × 22	W16 × 26	W6 × 20
	5–6	3	W12 × 26	W14 × 48	W16 × 26	W6 × 20
	7–8	4	W18 × 35	W14 × 48	W21 × 50	W18 × 50
	9–10	5	W21 × 44	W30 × 90	W30 × 90	W16 × 67
	11–12	6	W12 × 26	W30 × 99	W30 × 108	W16 × 67
	13–14	7	W18 × 35	W16 × 26	W14 × 22	W16 × 31
	15–16	8	W16 × 36	W12 × 16	W16 × 26	W12 × 30
	17–18	9	W16 × 36	W21 × 50	W21 × 50	W16 × 57
	19–20	10	W10 × 33	W6 × 20	W10 × 22	W10 × 22
Interior beam	1–2	11	W24 × 62	W18 × 40	W30 × 99	W16 × 77
	3–4	12	W16 × 40	W30 × 99	W30 × 90	W21 × 62
	5–6	13	W30 × 108	W24 × 62	W24 × 62	W18 × 60
	7–8	14	W16 × 50	W24 × 62	W24 × 62	W21 × 62
	9–10	15	W16 × 50	W14 × 43	W24 × 55	W24 × 62
	11–12	16	W18 × 60	W10 × 30	W18 × 40	W18 × 40
	13–14	17	W21 × 44	W21 × 73	W10 × 30	W16 × 36
	15–16	18	W16 × 36	W21 × 44	W14 × 22	W16 × 26
	17–18	19	W14 × 34	W16 × 26	W12 × 22	W10 × 22
	19–20	20	W14 × 30	W16 × 26	W14 × 22	W10 × 22
Corner Column	1–2	21	W12 × 106	W40 × 215	W40 × 199	W44 × 262
	3–4	22	W30 × 90	W40 × 183	W33 × 221	W33 × 221
	5–6	23	W18 × 97	W18 × 175	W27 × 129	W27 × 129
	7–8	24	W14 × 90	W24 × 162	W21 × 111	W18 × 106
	9–10	25	W14 × 109	W21 × 93	W21 × 111	W24 × 146
	11–12	26	W12 × 72	W21 × 166	W21 × 111	W24 × 146
	13–14	27	W14 × 90	W18 × 97	W18 × 97	W18 × 97
	15–16	28	W14 × 90	W14 × 90	W12 × 136	W18 × 97
	17–18	29	W10 × 39	W30 × 132	W12 × 136	W14 × 74
	19–20	30	W10 × 33	W8 × 28	W8 × 31	W8 × 31
Exterior Column	1–2	31	W14 × 233	W33 × 201	W33 × 221	W33 × 221
	3–4	32	W14 × 211	W33 × 201	W27 × 178	W27 × 178

Table 3 continued

Members	Story no.	Group no.	Hasancebi et al. [48]	Present work		
				FA	BBO	FABBO
	5–6	33	W14 × 211	W24 × 146	W27 × 146	W24 × 162
	7–8	34	W21 × 166	W24 × 146	W14 × 159	W18 × 175
	9–10	35	W14 × 132	W24 × 146	W27 × 178	W24 × 146
	11–12	36	W14 × 120	W21 × 93	W30 × 99	W27 × 102
	13–14	37	W12 × 106	W14 × 90	W14 × 90	W14 × 74
	15–16	38	W14 × 74	W12 × 87	W12 × 87	W21 × 68
	17–18	39	W12 × 58	W12 × 58	W14 × 53	W14 × 53
	19–20	40	W10 × 49	W10 × 17	W6 × 16	W6 × 25
Interior Column	1–2	41	W40 × 362	W40 × 215	W40 × 215	W27 × 235
	3–4	42	W40 × 268	W40 × 199	W27 × 217	W33 × 221
	5–6	43	W44 × 244	W36 × 194	W27 × 217	W33 × 221
	7–8	44	W44 × 244	W21 × 111	W36 × 135	W27 × 129
	9–10	45	W40 × 221	W12 × 152	W27 × 129	W30 × 99
	11–12	46	W40 × 149	W30 × 124	W24 × 104	W24 × 104
	13–14	47	W18 × 106	W21 × 93	W30 × 99	W18 × 106
	15–16	48	W30 × 99	W16 × 77	W16 × 67	W18 × 106
	17–18	49	W24 × 62	W18 × 76	W21 × 62	W21 × 50
	19–20	50	W16 × 36	W14 × 30	W5 × 19	W6 × 25
Bracing	1–2	51	W12 × 40	W18 × 35	W18 × 35	W8 × 31
	3–4	52	W8 × 40	W18 × 35	W18 × 35	W8 × 31
	5–6	53	W8 × 31	W21 × 44	W16 × 40	W8 × 31
	7–8	54	W12 × 26	W14 × 34	W16 × 40	W8 × 24
	9–10	55	W6 × 20	W16 × 26	W14 × 22	W8 × 24
	11–12	56	W10 × 22	W14 × 30	W12 × 16	W8 × 18
	13–14	57	W6 × 15	W8 × 24	W6 × 16	W5 × 19
	15–16	58	W6 × 15	W12 × 26	W6 × 20	W5 × 19
	17–18	59	W4 × 13	W8 × 21	W6 × 16	W5 × 19
	19–20	60	W4 × 13	W8 × 13	W6 × 9	W4 × 13
Weight (ton)			412.91	432.86	427.96	406.13
Number of analyses			60,000	20,000	20,000	20,000

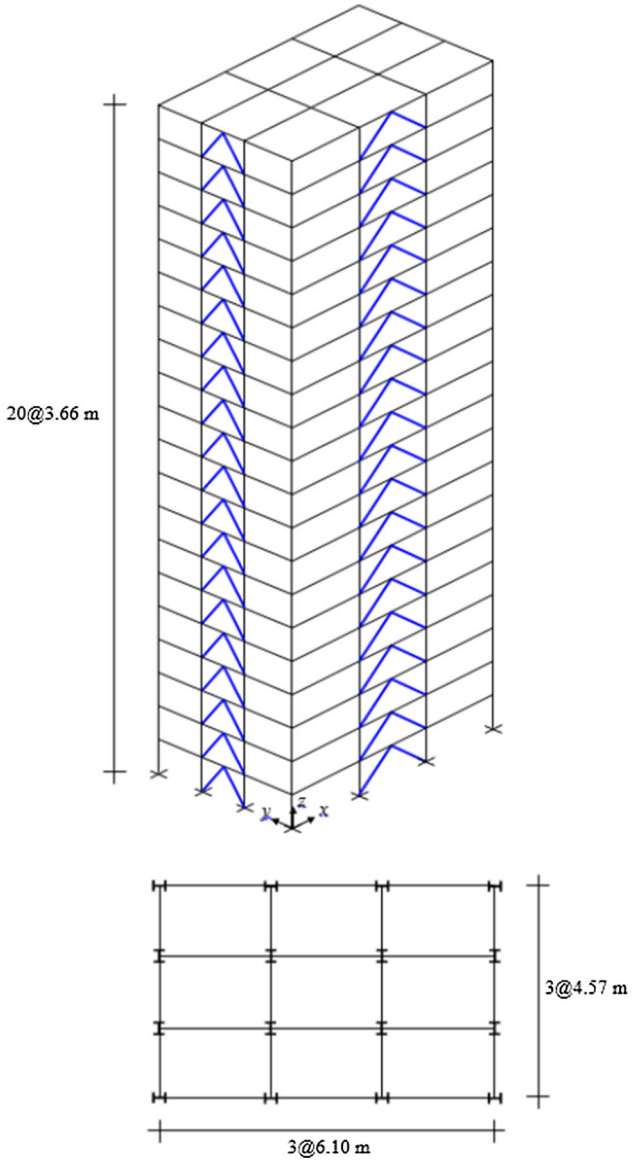

Fig. 11 20-story 3D steel frame

The optimum solution for the weight based on FA–BBO is 406.13 ton performing 20000 analyses, which is lighter than 412.91 ton reported in [48] conducting 60,000 analyses. Moreover, the results show that FA–BBO finds a solution which is 6.17% and 5.1% lighter than the solutions found by FA and BBO, respectively. Figures 12 and 13 depict the inter-story drift ratio profile as well as the element stress ratios for the optimal solution of FA–BBO, respectively. These results demonstrate the feasibility of the optimal solution.

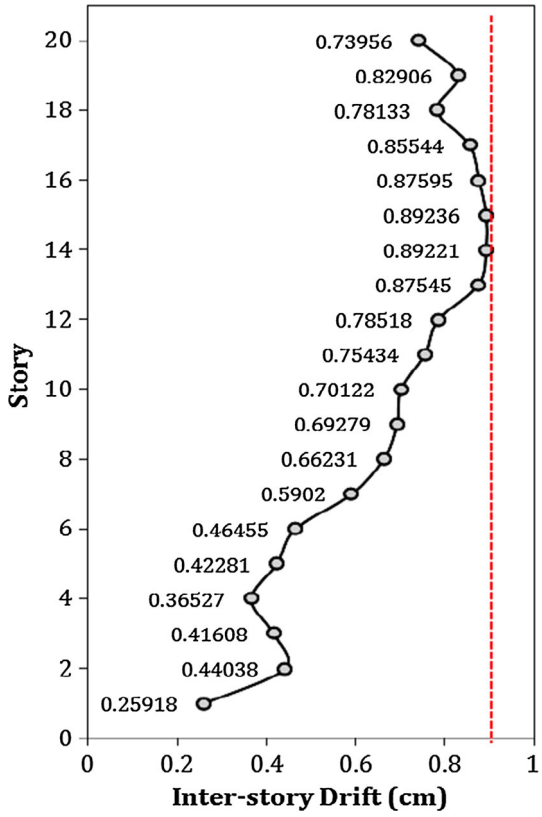

Fig. 12 Inter-story drift profile for optimal 20-story 3D steel frame based on FA–BBO

5 Conclusions

In the present study, a combined meta-heuristic algorithm is represented for the design optimization of SF structures. In this case, the main characteristics of FA and BBO optimization algorithms are combined and the resulted algorithm is termed as FA–BBO meta-heuristic. In this algorithm, FA acts as an explorer while the exploitation task is achieved by BBO. In other words, BBO performs a finer search around the solution found by FA. Three SF optimization examples are represented to demonstrate the computational superiority of the presented meta-heuristic algorithm. In each design examples, the results of FA–BBO are compared with other algorithms proposed in other studies. In all examples, the weight of the optimal structure found by FA–BBO is lighter compared with those of the other algorithms. Furthermore, the rate for the convergence of the FA–BBO is better than those of FA and BBO. Finally, it can be carried out that FA–BBO is an efficient meta-heuristic algorithm for the optimization of SF structures.

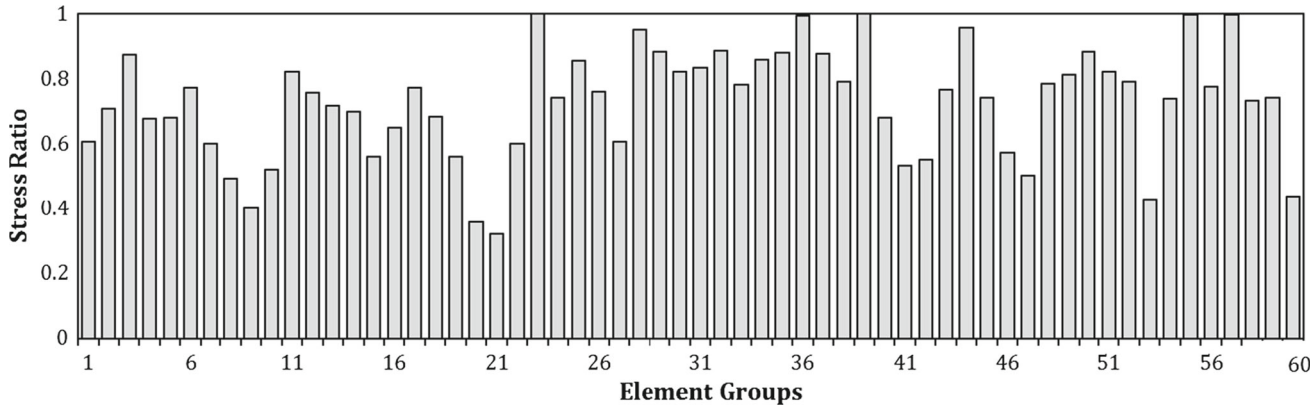

Fig. 13 Element group stress ratios for optimal 20-story 3D steel frame based on FA–BBO

References

1. Kaveh, A.; Talatahari, S.: Charged system search for optimal design of frame structures. Appl. Soft Comput. **12**(1), 382–393 (2012). https://doi.org/10.1016/j.asoc.2011.08.034
2. Kaveh, A.; Kalateh-Ahani, M.; Fahimi-Farzam, M.: Life-cycle cost optimization of steel moment-frame structures: performance-based seismic design approach. Earthq. Struct. **7**(3), 271–294 (2014). https://doi.org/10.12989/eas.2014.7.3.271
3. Kaveh, A.; Fahimi-Farzam, M.; Kalateh-Ahani, M.: Optimum design of steel frame structures considering construction cost and seismic damage. Smart Struct. Syst. **16**(1), 1–26 (2015). https://doi.org/10.12989/sss.2015.16.1.001
4. Nematzadeh, M.; Shahmansouri, A.A.; Fakoor, M.: Post-fire compressive strength of recycled PET aggregate concrete reinforced with steel fibers: optimization and prediction via RSM and GEP. Constr. Build. Mater. **252**, 119057 (2020). https://doi.org/10.1016/j.conbuildmat.2020.119057
5. Kaveh, A.; Eslamlou, A.D.: Performance-based multi-objective optimization of large steel structures. In: Metaheuristic Optimization Algorithms in Civil Engineering: New Applications. Studies in Computational Intelligence, vol. 900. Springer, Cham (2020). https://doi.org/10.1007/978-3-030-45473-9_8
6. Kaveh, A.; Kalateh-Ahani, M.; Fahimi-Farzam, M.: Damage-based optimization of large-scale steel structures. Earthq. Struct. **7**(6), 1119–1139 (2014). https://doi.org/10.12989/eas.2014.7.6.1119
7. Shahmansouri, A.A.; Bengar, H.A.; Ghanbari, S.: Compressive strength prediction of eco-efficient GGBS-based geopolymer concrete using GEP method. J. Build. Eng. (2020). https://doi.org/10.1016/j.jobe.2020.101326
8. Shahmansouri, A.; Bengar, H.A.; Ghanbari, S.: Experimental investigation and predictive modeling of compressive strength of pozzolanic geopolymer concrete using gene expression programming. J. Concr. Struct. Mater. (2020). https://doi.org/10.30478/jcsm.2020.214158.1141
9. Shahmansouri, A.A.; Yazdani, M.; Ghanbari, S.; Bengar, H.A.; Jafari, A.; Ghatte, H.F.: Artificial neural network model to predict the compressive strength of eco-friendly geopolymer concrete incorporating silica fume and natural zeolite. J. Clean. Prod. (2020). https://doi.org/10.1016/j.jclepro.2020.123697
10. Zou, D.; Liu, H.; Gao, L.; Li, S.: A novel modified differential evolution algorithm for constrained optimization problems. Comput. Math Appl. **61**(6), 1608–1623 (2011). https://doi.org/10.1016/j.camwa.2011.01.029
11. Gholizadeh, S., Barati, H.: A comparative study of three meta-heuristics for optimum design of trusses. (2012)
12. Zou, D.; Wu, J.; Gao, L.; Li, S.: A modified differential evolution algorithm for unconstrained optimization problems. Neurocomputing **120**, 469–481 (2013). https://doi.org/10.1016/j.neucom.2013.04.036
13. Fattahi, H.: Application of improved support vector regression model for prediction of deformation modulus of a rock mass. Eng. Comput. **32**(4), 567–580 (2016). https://doi.org/10.1007/s00366-016-0433-6
14. Lavalette, N.; Bergsma, O.; Zarouchas, D.; Benedictus, R.: Comparative study of adhesive joint designs for composite trusses based on numerical models. Appl. Adhes. Sci. **5**(1), 1–20 (2017). https://doi.org/10.1186/s40563-017-0100-1
15. Kaveh, A.; Kabir, M.; Bohlool, M.: Optimum design of three-dimensional steel frames with prismatic and non-prismatic elements. Eng. Comput. (2019). https://doi.org/10.1007/s00366-019-00746-9
16. Cicconi, P.; Castorani, V.; Germani, M.; Mandolini, M.; Vita, A.: A multi-objective sequential method for manufacturing cost and structural optimization of modular steel towers. Eng. Comput. **36**(2), 475–497 (2020). https://doi.org/10.1007/s00366-019-00709-0
17. Gholizadeh, S.; Hassanzadeh, A.; Milany, A.; Ghatte, H.F.: On the seismic collapse capacity of optimally designed steel braced frames. Eng. Comput. (2020). https://doi.org/10.1007/s00366-020-01096-7
18. Sotiropoulos, S.; Kazakis, G.; Lagaros, N.D.: Conceptual design of structural systems based on topology optimization and prefabricated components. Comput. Struct. **226**, 106136 (2020). https://doi.org/10.1016/j.compstruc.2019.106136
19. Kaveh, A.; Azar, B.F.; Hadidi, A.; Sorochi, F.R.; Talatahari, S.: Performance-based seismic design of steel frames using ant colony optimization. J. Constr. Steel Res. **66**(4), 566–574 (2010). https://doi.org/10.1016/j.jcsr.2009.11.006
20. Kaveh, A.; Laknejadi, K.; Alinejad, B.: Performance-based multi-objective optimization of large steel structures. Acta Mech. **223**(2), 355–369 (2012). https://doi.org/10.1007/s00707-011-0564-1
21. Kaveh, A.; Nasrollahi, A.: Performance-based seismic design of steel frames utilizing charged system search optimization. Appl. Soft Comput. **22**, 213–221 (2014). https://doi.org/10.1016/j.asoc.2014.05.012
22. Kaveh, A.; Talatahari, S.: An improved ant colony optimization for the design of planar steel frames. Eng. Struct. **32**(3), 864–873 (2010). https://doi.org/10.1016/j.engstruct.2009.12.012
23. Kaveh, A.; Zakian, P.: Optimal design of steel frames under seismic loading using two meta-heuristic algorithms. J. Constr. Steel Res. **82**, 111–130 (2013). https://doi.org/10.1016/j.jcsr.2012.12.003

24. Kaveh, A.; Bakhshpoori, T.: Optimum design of steel frames using Cuckoo Search algorithm with Lévy flights. Struct. Des. Tall Spec. Build. **22**(13), 1023–1036 (2013). https://doi.org/10.1002/tal.754
25. Kaveh, A.; BolandGerami, A.: Optimal design of large-scale space steel frames using cascade enhanced colliding body optimization. Struct. Multidiscip. Optim. **55**(1), 237–256 (2017). https://doi.org/10.1007/s00158-016-1494-2
26. Kaveh, A.; Ilchi Ghazaan, M.: Optimum seismic design of 3D irregular steel frames using recently developed metaheuristic algorithms. J. Comput. Civ. Eng. **32**(3), 04018015 (2018). https://doi.org/10.1061/(ASCE)CP.1943-5487.0000760
27. Yang, X.-S.: Firefly algorithms for multimodal optimization. In: International symposium on stochastic algorithms 2009, pp. 169–178. Springer
28. Simon, D.: Biogeography-based optimization. IEEE Trans. Evol. Comput. **12**(6), 702–713 (2008). https://doi.org/10.1109/TEVC.2008.919004
29. LRFD, A.: Manual of steel construction, load and resistance factor design. In: Chicago: American Institute of Steel Construction. AISC, Chicago, IL, USA (1994)
30. Vanderplaats, G.N.; Vanderplaats, G.: Numerical Optimization Techniques for Engineering Design: With Applications. McGraw-Hill, New York (1984)
31. Yang, X.-S.: Nature-Inspired Metaheuristic Algorithms. Luniver Press, Beckington (2010)
32. Gandomi, A.H.; Yang, X.-S.; Alavi, A.H.: Mixed variable structural optimization using firefly algorithm. Comput. Struct. **89**(23–24), 2325–2336 (2011). https://doi.org/10.1016/j.compstruc.2011.08.002
33. Pan, Y.; Chen, L.; Wang, J.; Ma, H.; Cai, S.; Pu, S.; Duan, J.; Gao, L.; Li, E.: Research on deformation prediction of tunnel surrounding rock using the model combining firefly algorithm and nonlinear auto-regressive dynamic neural network. Eng. Comput. (2019). https://doi.org/10.1007/s00366-019-00894-y
34. Zhou, J.; Nekouie, A.; Arslan, C.A.; Pham, B.T.; Hasanipanah, M.: Novel approach for forecasting the blast-induced AOp using a hybrid fuzzy system and firefly algorithm. Eng. Comput. (2019). https://doi.org/10.1007/s00366-019-00725-0
35. Kaur, M.; Ghosh, S.: Network reconfiguration of unbalanced distribution networks using fuzzy-firefly algorithm. Appl. Soft Comput. **49**, 868–886 (2016). https://doi.org/10.1016/j.asoc.2016.09.019
36. Zhang, Y.; Wu, L.: A novel method for rigid image registration based on firefly algorithm. Int. J. Res. Rev. Soft Intell. Comput. **2**(2), 141–146 (2012)
37. Apostolopoulos, T.; Vlachos, A.: Application of the firefly algorithm for solving the economic emissions load dispatch problem. Int. J. Combin. (2010). https://doi.org/10.1155/2011/523806
38. Basu, B.; Mahanti, G.K.: Fire fly and artificial bees colony algorithm for synthesis of scanned and broadside linear array antenna. Prog. Electromagn. Res. **32**, 169–190 (2011). https://doi.org/10.2528/pierb11053108
39. Jakimovski, B., Meyer, B., Maehle, E.: Firefly flashing synchronization as inspiration for self-synchronization of walking robot gait patterns using a decentralized robot control architecture. In: International conference on architecture of computing systems 2010, pp. 61–72. Springer
40. Gordan, B.; Koopialipoor, M.; Clementking, A.; Tootoonchi, H.; Mohamad, E.T.: Estimating and optimizing safety factors of retaining wall through neural network and bee colony techniques. Eng. Comput. **35**(3), 945–954 (2019). https://doi.org/10.1007/s00366-018-0642-2
41. Moayedi, H.; Nguyen, H.; Rashid, A.S.A.: Novel metaheuristic classification approach in developing mathematical model-based solutions predicting failure in shallow footing. Eng. Comput. (2019). https://doi.org/10.1007/s00366-019-00819-9
42. Yuan, C.; Moayedi, H.: The performance of six neural-evolutionary classification techniques combined with multi-layer perception in two-layered cohesive slope stability analysis and failure recognition. Eng. Comput. (2019). https://doi.org/10.1007/s00366-019-00791-4
43. Mirjalili, S.; Mirjalili, S.M.; Lewis, A.: Let a biogeography-based optimizer train your multi-layer perceptron. Inf. Sci. **269**, 188–209 (2014). https://doi.org/10.1016/j.ins.2014.01.038
44. García-Torres, J.M.; Damas, S.; Cordón, O.; Santamaría, J.: A case study of innovative population-based algorithms in 3D modeling: artificial bee colony, biogeography-based optimization, harmony search. Expert Syst. Appl. **41**(4), 1750–1762 (2014). https://doi.org/10.1016/j.eswa.2013.08.074
45. Pezeshk, S.; Camp, C.; Chen, D.: Design of nonlinear framed structures using genetic optimization. J. Struct. Eng. **126**(3), 382–388 (2000). https://doi.org/10.1061/(ASCE)0733-9445(2000)126:3(382)
46. Camp, C.V.; Bichon, B.J.; Stovall, S.P.: Design of steel frames using ant colony optimization. J. Struct. Eng. **131**(3), 369–379 (2005). https://doi.org/10.1061/(ASCE)0733-9445(2005)131:3(369)
47. Degertekin, S.O.: Optimum design of steel frames using harmony search algorithm. Struct. Multidiscip. Optim. **36**(4), 393–401 (2008). https://doi.org/10.1007/s00158-007-0177-4
48. Hasançebi, O.; Bahçecioğlu, T.; Kurç, Ö.; Saka, M.: Optimum design of high-rise steel buildings using an evolution strategy integrated parallel algorithm. Comput. Struct. **89**(21–22), 2037–2051 (2011). https://doi.org/10.1016/j.compstruc.2011.05.019
49. ASD, A.: Manual of steel construction. In: Chicago: American Institute of Steel Construction. AISC, Chicago, Illinois, USA (1989)
50. ASCE 7-05: Minimum design loads for building and other structures. In: ASCE (2005)